Bull. Mater. Sci., Vol. 34, No. 1, February 2011, pp. 133–142. © Indian Academy of Sciences.

Dielectric response of PLZT ceramics *x*/57/43 across ferroelectric–paraelectric phase transition

A K SHUKLA[1,2,*], V K AGRAWAL[1], I M L DAS[1], JANARDAN SINGH[3] and S L SRIVASTAVA[1]

[1]Department of Physics, University of Allahabad, Allahabad 211 002, India
[2]Department of Physics, Amity Institute of Applied Sciences, Amity University, Noida 201 301, India
[3]National Physical Laboratory, Dr K S Krishnan Road, New Delhi 110 012, India

MS received 21 July 2009; revised 21 July 2010

Abstract. **The dielectric properties of lead lanthanum zirconate titanate (PLZT) ceramics [$Pb(Zr_{0.57}Ti_{0.43})O_3 + x$ at% of La, $x = 3$, 5, 6, 10 and 12] have been measured in the frequency range 1 Hz–1 MHz using the vector impedance spectroscopy (VIS) at different temperatures. All the compositions show both non-dispersive and dispersive dielectric responses in different temperature regions. The non-dispersive region obeys the universal dielectric response. A low frequency (<1 kHz) relaxation phenomenon with a high value of distribution parameter '*h*' (~0·4 to 0·6) has been observed in all the compositions around the temperature corresponding to the maximum dielectric constant (T_m). The activation energies as calculated from the relaxation and d.c. conduction processes are comparable. The ferroelectric phase transition is diffuse in nature and broadening of the peak increases with La content.**

Keywords. **PLZT; dielectric relaxation; diffuse phase transition.**

1. Introduction

The La-doped lead zirconate titanate (PLZT) piezoelectric ceramics have been used for the transducer as well as in the actuator devices (Haertling 1999; Uchino 2008). Apart from the technological applications, the PLZT ceramics show normal ferroelectric phase transition to relaxor characteristics in a series of compositions by varying the La concentration in the base lead zirconate titanate (PZT) systems (Dai *et al* 1994). Shemin *et al* (1988) reported the domain-like transition in PLZT under d.c. bias. Dai *et al* (1993) observed that small La content can diffuse the dielectric response in the temperature region around phase transition in tetragonal PLZTs. The relaxor to normal ferroelectric transition has been attributed to a local to global symmetry transition by them. Dellis *et al* (1994) considered PLZT ceramics as superparaelectric glass, evidenced from its relaxation behaviour. The a.c. field dependence of dielectric constant for PLZT *x*/65/35 has been performed by Tan and Viehland (1996). They reported that strong nonlinearity and large shifts in transition temperatures for certain compositions decrease at higher La concentrations. The coexistence of normal and relaxor phases in compositions close to MPB has been observed by Gupta *et al* (1998) who reported that the degree of polar order in PLZT continues to decrease with La. Based on dielectric and Raman spectroscopic study, Marssi *et al* (1998) concluded the PLZTs *x*/65/35 as a model of cluster of glass with short range ordered polar clusters rather than a multidomain state. Lin *et al* (1999) used a multi Debye relaxation model, based upon Boltzmann superposition principle to determine relaxation time spectra quantitatively for PLZT 8/65/35. Freezing of dynamic process in PLZT 9/65/35 has been studied by Kutnjak *et al* (1999) by analysing field cooled (FC) and zero field cooled (ZFC) dielectric spectra. They have reported that for an aged PLZT sample, the ergodicity is broken due to the divergence of the longest relaxation time in the vicinity of temperature where ferroelectric phase can also be induced under application of sufficient d.c. electric field. The dielectric behaviour of PLZT 8, 9·5/65/35 in a very wide range of frequency (20 Hz–100 THz) and temperature (10 K–530 K) has been studied by Kamba *et al* (2000) followed by study of distribution of relaxation times by Kajokas *et al* (2001). They reported that mean relaxation time diverges according to Vogel–Fulcher law. They have also shown that loss spectra become frequency independent below room temperature and permittivity increases linearly with logarithmic decrement of frequency. On the basis of a phenomenological model with restricted drift motion of charged particles, Volkov *et al* (2003) described the universal dynamic response and broad band relaxation considering Maxwell–Wagner type interaction between conducting clusters of relaxors like PLZTs. The room temperature dielectric response of PLZT *x*/57/43 and Cr-doped PLZT 6/57/43 and temperature dependent piezoelectric response of PLZT *x*/57/43 have been investigated by us and it is found that the a.c. conductivity of these compositions follows the universal dielectric response

*Author for correspondence (akshukla@amity.edu)

(Jonscher 1977; Shukla *et al* 2004, 2006, 2010). Reviews by Buixaderas *et al* (2004) and Bokov and Ye (2006) describe various features of perovskite relaxors such as PLZTs and a variety of observations are attributed to the presence of polar nanoregions in the material.

From the above reviews, we find that extensive research has been carried out on the ferroelectric phase transition of PLZTs mostly on the composition *x*/65/35. However, the data on ferroelectric phase transition in the vicinity of morphotropic phase boundary (MPB) region and other compositions are rather scarce. Also the systematic study on universal dielectric response of PLZTs across the ferroelectric phase transition region is still lacking. In the present work, we report the ferroelectric phase transition of PLZT *x*/57/43 using the vector impedance spectroscopy (VIS).

2. Experimental

The compositions of La-doped PZT [$Pb(Zr_{0.57}Ti_{0.43})O_3 + x$ at% of La, where $x = 3$, 5, 6, 10 and 12] have been synthesized using mixed oxide method. Two weight percent of excess lead oxide was added in the compositions to compensate the lead loss during sintering. Samples of various compositions have been homogenized in acetone medium using agate mortar and pestle, calcined at 900°C for about half an hour, rehomogenized and finally sintered under lead atmosphere in disc form at 1200°C for 2 h. The details of sample preparation and poling have been discussed by us earlier (Shukla *et al* 2004, 2006). The poled disc shaped specimens of these compositions have been used for measurement. The temperature dependent measurements of real and imaginary parts of dielectric constants, ε' and ε'', have been performed using a computer controlled Solartron 1260 Impedance Gain Phase analyzer coupled with Solartron 1296 dielectric interface in the frequency range 1 Hz–1 MHz with rms a.c. voltage 0·5 V, heating them from *RT* to 400°C.

3. Results and discussion

The typical plots of real and imaginary parts of dielectric constants, ε' and ε'', with temperature at selected frequencies are shown in figure 1 and it is observed that for a given composition, maximum value of the dielectric constant decreases with increase in frequency. The rounded maximum in the dielectric peak is the signature of diffuse type ferroelectric–paraelectric phase transition. Such roundedness maxima are seen in all the compositions and broadening in the dielectric data at T_m (temperature corresponding to the maximum dielectric constant for a given composition) increases with increase in La concentration and that T_m does not change with frequency. It is also seen that ε'' increases sharply beyond T_m in all samples which may be because of high concentration of defects at higher temperatures (Marssi *et al* 1998). All the studied compositions show marked dielectric dispersion around ferroelectric–paraelectric phase transition region. As such two regions in dielectric data with temperature have been observed. These are the non-dispersive and dispersive regions with frequency, which are discussed separately in the following sections.

3.1 *Non-dispersive nature of ε' and ε'' of PLZTs*

Dielectric constant, ε' and conductivity, σ, of the PLZT material are fitted with universal dielectric behaviour within the frequency range of 1Hz – 10 kHz, using the following relations

$$\sigma(f) = \sigma_{dc} + Af^s, \quad \varepsilon'(f) = \varepsilon'_\infty + Bf^n,$$

where the exponents n and s add to 1 (Jonscher 1977; Lee *et al* 1991), A and B are fitting constants, σ_{dc} the d.c. conductivity and ε'_∞ the high frequency limiting value of the dielectric constant. The fitted exponents n and s are listed in table 1. $n \sim 0$ and $s \sim 1$ for all the samples except for $x = 10{\cdot}1$ at% La, for which $s \sim 0{\cdot}6$. The parameter 's' shows a decreasing trend and 'n' increases with temperature. A decrease in 's' has also been observed for glasses and ceramics (Lee *et al* 1991). Although $n + s$ should be 1 as a consequence of Kramer–Kronig relation, however, it is slightly higher than 1. $s > 1$ has also been reported in high frequency region (MHz – microwave) for other solid systems possessing non-Arrhenius d.c. conductivity and attributed to the hopping of ions through localized states (Lakatos and Abkowitz 1971; Durand *et al* 1994; Cramer and Buscher 1998; Dyre and Schroder 2000).

3.2 *Dispersive nature of ε' and ε'' of PLZTs*

The dispersion region is analysed through the following generalized Cole–Cole equations (Cole and Cole 1942; Shukla 2007)

$$\varepsilon' = \frac{A_1}{f^n} + \varepsilon'_\infty + \Delta\varepsilon \frac{1 + \left(\frac{f}{f_R}\right)^{1-h} \sin\left(\frac{h\pi}{2}\right)}{1 + 2\left(\frac{f}{f_R}\right)^{1-h} \sin\left(\frac{h\pi}{2}\right) + \left(\frac{f}{f_R}\right)^{2(1-h)}}, \tag{1}$$

$$\varepsilon'' = \frac{A_2}{f^m} + \Delta\varepsilon \frac{\left(\frac{f}{f_R}\right)^{1-h} \cos\left(\frac{h\pi}{2}\right)}{1 + 2\left(\frac{f}{f_R}\right)^{1-h} \sin\left(\frac{h\pi}{2}\right) + \left(\frac{f}{f_R}\right)^{2(1-h)}} + A_3 f^{m1}, \tag{2}$$

here $\Delta\varepsilon = \varepsilon'_0 - \varepsilon'_\infty$ is known as the dielectric strength of the material, ε'_0 the static dielectric constant, f_R the relaxation frequency and h the distribution parameter. A_1, A_2, A_3, n, m and $m1$ are the fitting parameters. The first terms in (1) and (2) represent the low frequency correction and the third term in (2) represents the high frequency correction term.

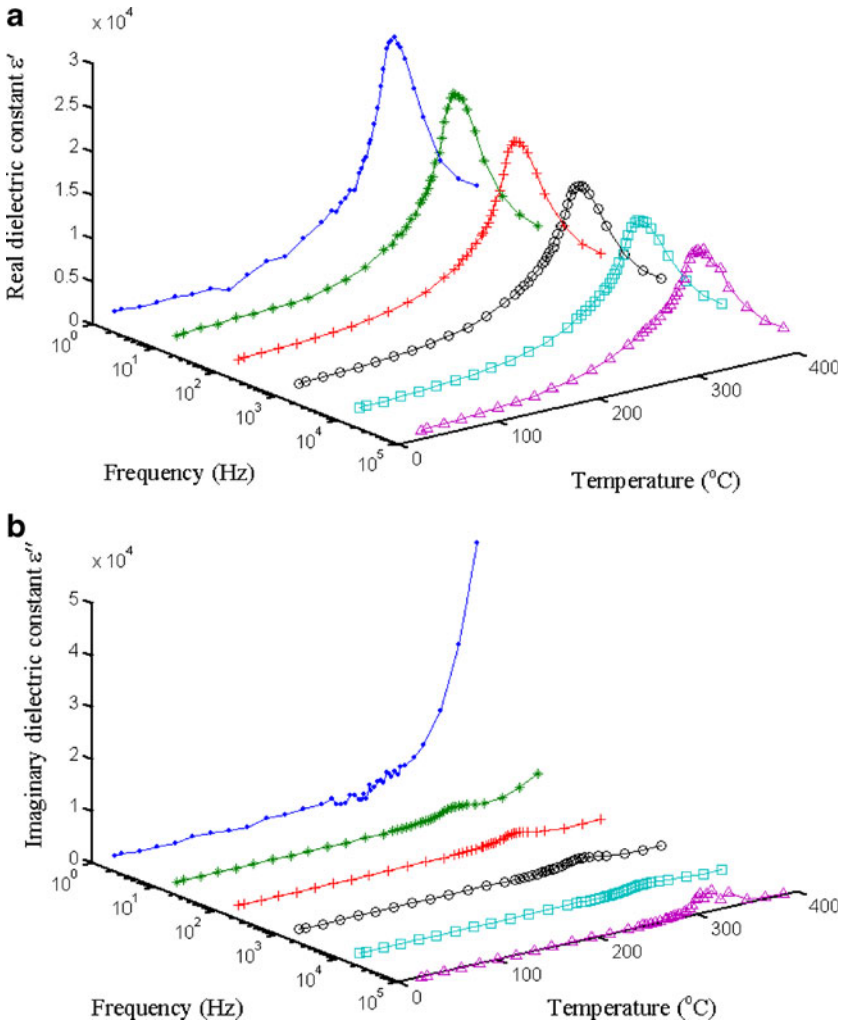

Figure 1. Variation of the real and imaginary parts of the dielectric constant with temperature at selected frequencies for $x = 3{\cdot}0$ at% of La.

Table 1. Variation of exponents, n and s, at different temperatures for $x = 6{\cdot}0$ and $10{\cdot}1$ at% of La.

$x = 6{\cdot}0$ at% of La			$x = 10{\cdot}1$ at% of La		
T (°C)	n	s	T (°C)	n	s
28	0·07	1·02	25	0·34	0·60
44	0·06	1·01	29	0·35	0·63
62	0·08	1·01	46	0·36	0·79
80	0·06	0·97	81	0·07	1·01
98	0·09	0·94	100	0·06	0·96
116	0·10	0·90	116	0·15	0·93
134	0·15	0·87	138	0·22	0·85
190	0·26	0·77	296	0·33	0·74
199	0·31	0·76	313	0·46	0·65
347	0·17	0·87	331	0·43	0·57
367	0·16	0·93	350	0·44	0·54
383	0·20	0·98	370	0·44	0·54
–	–	–	388	0·42	0·52

ε' and ε'' show frequency dependence following (1) and (2) for all the samples around T_m, except for $x = 12{\cdot}1$ at% of La, for which the Cole–Cole dispersion behaviour shifts to the paraelectric phase. The fitted and experimental data of ε' and ε'' along with low and high frequency corrections are shown in figure 2. The dielectric data has been refined by subtracting the value of low frequency dependent part from the experimental data and thereafter the Cole–Cole terms (third from (1) and second from (2)) are analysed. It is found that ε'_∞ are very close to the ε' at 10 kHz for all the samples. The variation of experimental dielectric data and ε'_∞ for one sample has been shown in figures 3(a) and (b), respectively.

The high frequency limiting value of dielectric constant, ε'_∞, is used for the study of ferroelectric–paraelectric phase transition behaviour. The values of dielectric strength, $\Delta\varepsilon$, static dielectric constant, ε'_0, relaxation frequency, f_R and distribution parameter, h, at the transition temperature, T_m, are given in table 2. Discontinuities in $\Delta\varepsilon$ and ε'_0 are observed at the transition temperature, T_m, for $x = 10{\cdot}1$ at%

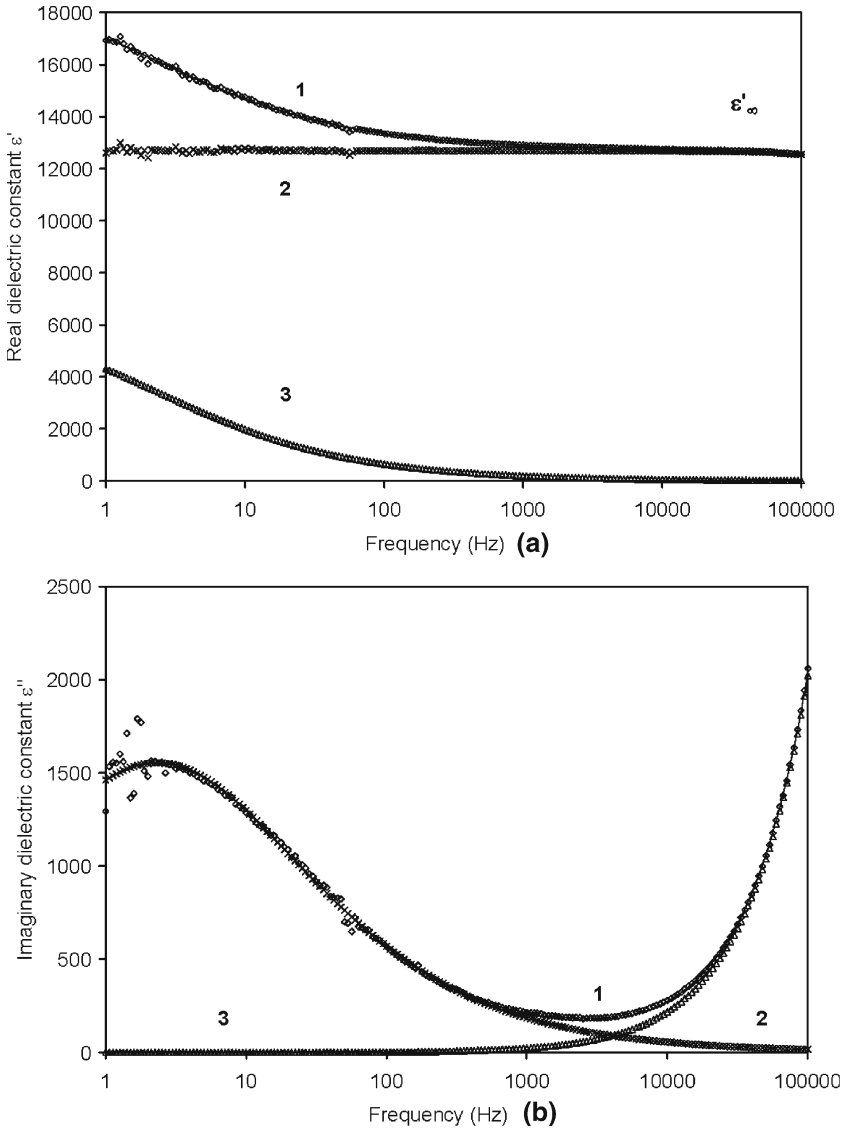

Figure 2. (**a**) Real part of dielectric constant showing dispersion near 1Hz for $x = 6{\cdot}0$ at% of La, at 227·27°C. Curve 1 in the figure represents the experimental data along with best fitted solid line. Curve '2' represents the corrected dielectric constant after subtracting Cole–Cole term from experimental data of ε'. Curve 3 represents Cole–Cole term and (**b**) imaginary part of dielectric constant corresponding to $x = 6{\cdot}0$ at% of La. Curve 1 in the figure represents the experimental data along with best fitted data represented by solid line. Curves 2 and 3 represent the Cole–Cole term and high frequency correction term, respectively.

of La. The temperature dependence of the dielectric constants, ε'_∞ (figure 4), shows a La concentration dependent broadened peak. The peak temperature, T_m, decreases with La in PZT perovskite structure. The high values of symmetric distribution parameter, h, reveal broad dielectric dispersion in the material. Kamba *et al* (2000) also reported high values of h (∼0·85 for PLZT 9·5/65/35, ∼0·8 for PLZT 8/65/35 around room temperature and 70°C, respectively) which decreases with increase in temperature and explained the dielectric response on the basis of temperature dependence of size distribution of polar regions, fluctuation of their amplitudes and the dipole fluctuation among them. High value of h (∼0·4) has also been observed by Kirillov and Isupov (1973) for lead magnesium niobate (PMN) and attributed it to the existence of polar region within non-polar region.

The Cole–Cole dispersion behaviours are observed between 150 and 350°C for all the samples. The width of

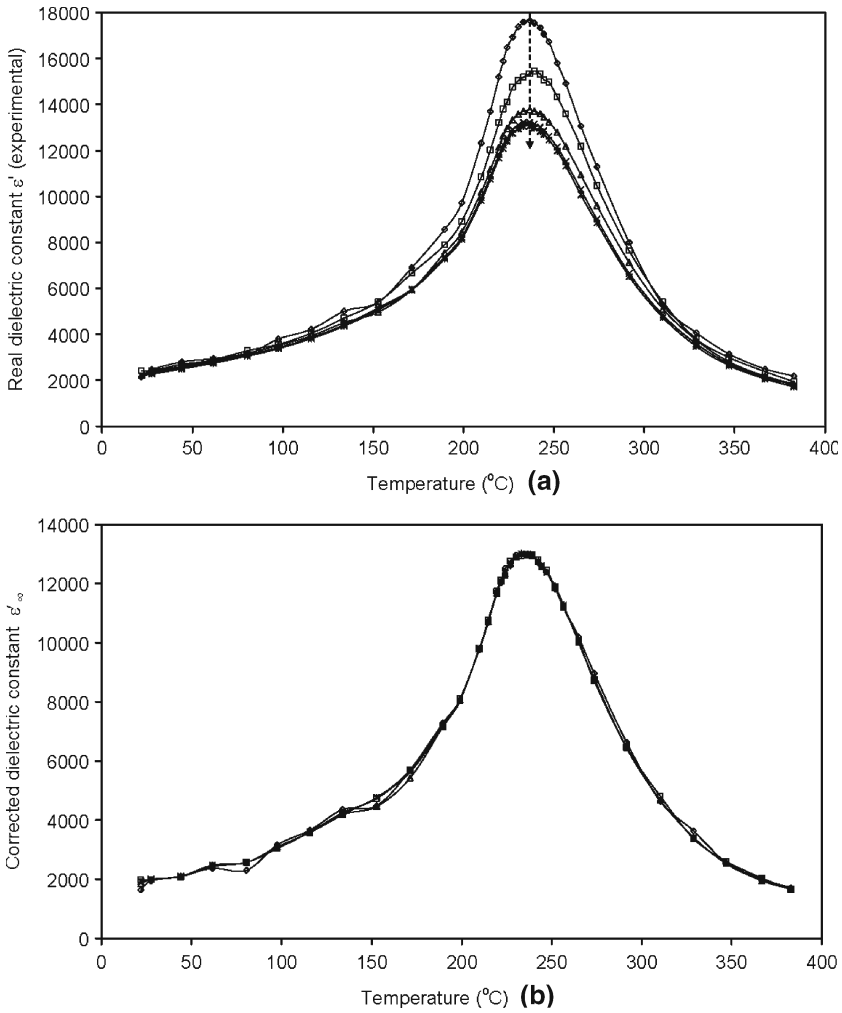

Figure 3. Behaviour of the real part of the dielectric constant with temperature: (**a**) experimental data of dielectric constant corresponding to 1, 10, 100, 1000 and 10000 Hz, and (**b**) corrected data of dielectric constant at same frequencies. Arrow in 3(a) indicates the increasing direction of frequency at peak dielectric constant value. The data presented in this figure corresponds to $x = 6{\cdot}0$ at% of La.

Table 2. Values of transition temperature, T_m and static dielectric constant, ε'_0, dielectric strength, $\Delta\varepsilon$, distribution parameter, h, and relaxation frequency, f_R, at T_m for different compositions of PLZT except for $x = 12{\cdot}1$ at% of La at which these parameters are at 198°C in the paraelectric region.

x (at% of La)	T_m (°C)	ε'_0	$\Delta\varepsilon$	h	f_R (Hz)
3·0	300	$2{\cdot}16\times10^4$	$6{\cdot}90\times10^3$	0·44	157·41
5·0	256	$2{\cdot}07\times10^4$	$6{\cdot}83\times10^3$	0·46	7·42
6·0	233	$1{\cdot}94\times10^4$	$6{\cdot}35\times10^3$	0·45	3·48
10·1	196	$0{\cdot}71\times10^4$	$0{\cdot}97\times10^3$	0·53	35·59
12·1	143	$0{\cdot}75\times10^4$	$0{\cdot}16\times10^3$	0·53	2·49

the dispersion region varies with La concentration on the temperature scale. It is also observed that h increases sharply with temperature for $x = 10{\cdot}1$ at% of La, and shows a discontinuity at the transition temperature. However, all samples show a similar Cole–Cole behaviour in the paraelectric region. Overall the value of h is confined in between 0·6 – 0·4 and weak temperature dependence is observed. The value of h decreases initially with temperature and thereafter becomes almost constant.

The relaxation frequency, f_R, increases with increasing temperature. The relaxation frequencies follow the Arrhenius behaviour, $f_R = f_0 \exp\left(-\frac{E_a}{kT}\right)$, where f_0 is an attempt to jump frequency, E_a the activation energy for relaxation process, k the Boltzmann constant and T the absolute temperature. Plots of $\ln(f_R)$ vs $1/T$ (K) are shown in figure 5.

No change of slope through the ferroelectric to paraelectric phase transition is observed for $x = 3$, 5 and 6 at%. For $x = 10{\cdot}1$ at% of La, a discontinuity in f_R is found at T_m.

The d.c. conductivity also follows the Arrhenius behaviour, $\sigma_{dc} = \sigma_0 \exp\left(-\frac{E_a}{kT}\right)$, where σ_0 is a pre-exponential term and E_a corresponds here to the conduction activation energy. The Arrhenius plots of the d.c. conductivity in paraelectric region are shown in figure 6. The activation energies as calculated from the plots of f_R and d.c. conductivity for different compositions of PLZT are presented in table 3.

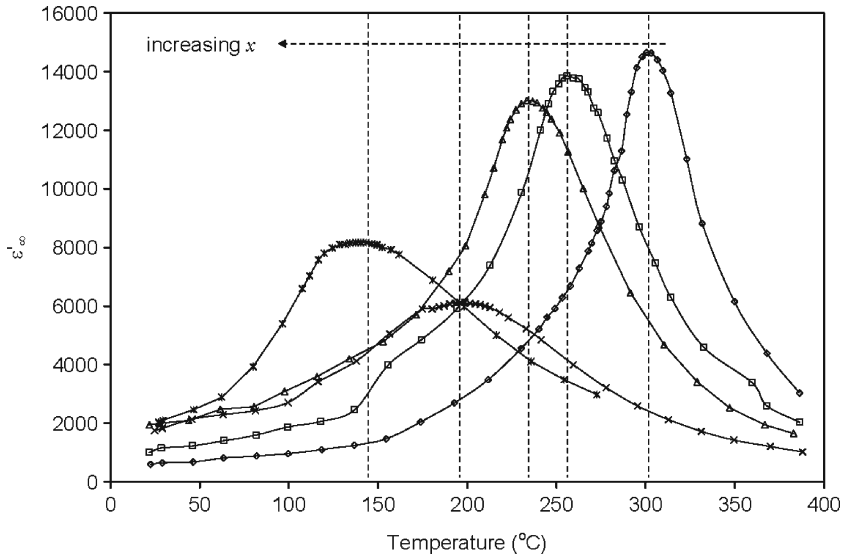

Figure 4. Change in the high frequency limiting value of the dielectric constant, ε'_∞, with temperature corresponding to different samples of PLZT. These values are determined from fitting of dielectric data in both non-dispersive and dispersive regions. The vertical lines correspond to the maximum dielectric constant with temperature, T_m, for respective compositions.

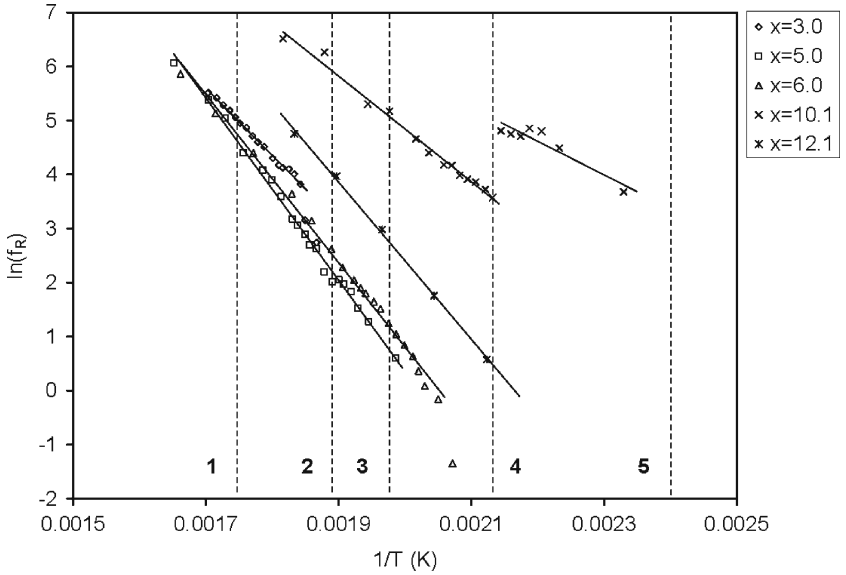

Figure 5. Arrhenius behaviour of relaxation frequency corresponding to different compositions. Vertical dotted lines 1, 2, 3, 4 and 5 represent the transition temperature, T_m, with increasing concentration, respectively.

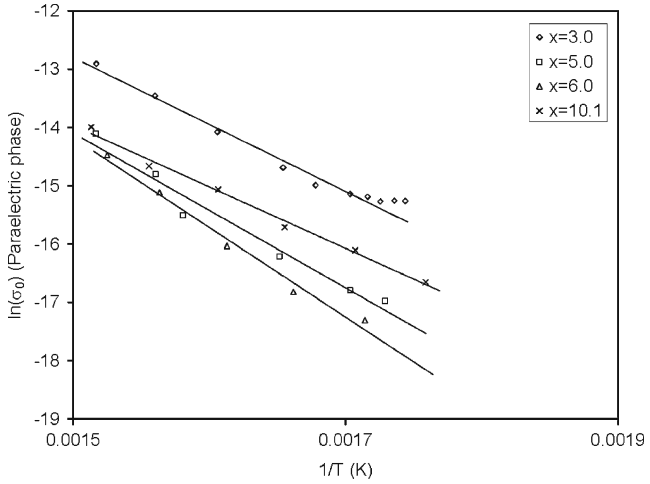

Figure 6. Arrhenius plot of d.c. conductivity in the paraelectric region for different compositions. The d.c. conductivity is determined from fitting of imaginary part of dielectric data in paraelectric region. It is very difficult to estimate the value of d.c. conductivity in ferroelectric region as d.c. conductivity is very low and also dispersion phenomenon starts at low frequency below transition region and spreads in several decades around peak frequency corresponding to ε''.

Table 3. Activation energy calculated from Arrhenius plot of f_R and σ_0 for different compositions.

x (at % of La)	$E_a(f_R)$ eV	$E_a(\sigma_0)$ eV
3·0	1·07	0·99
5·0	1·46	1·14
6·0	1·34	1·32
10·1	0·84	0·91
	0·54	–
12·1	1·26	–

The Debye type dispersion phenomenon in PLZT around T_m has been reported by Arora *et al* (1992) and Schmitt and Dorr (1989). The low frequency dielectric dispersion has also been reported for other perovskites (Bidault *et al* 1994; Ang *et al* 2000). They also reported that the activation energies for dielectric relaxation and conduction are comparable and represents the same physical nature. For La-doped lead titanate, Bidault *et al* (1994) proposed that a link between relaxation and conduction phenomenon is an indication of thermally activated space charge. They further assumed that (a) dipolar relaxation is due to the oxygen vacancies adjacent to Ti^{4+}, which may relax between six equivalent sites of unit cell, (b) the mobility of oxygen vacancy is extended to whole sample leading to the ionic conductivity, and (c) storage of free charge carriers at the two material–electrode interfaces, which leads to space charge effect. In fact, such a low frequency dielectric relaxation is very common in Ti-based ABO_3 perovskites (Ang *et al* 2000). The phenomenon of relaxation and conduction in Bi-doped strontium titanate has also been attributed to the ionization of oxygen vacancies (Ang *et al* 2000). According to Skanavi model (Bidault *et al* 1994 and references therein), small motion of Ti^{4+} ion can cause the reorientation of dipoles.

The temperature dependent phase transition occurs in the PZT based materials (near MPB region) via the transformation from rhombohedral–tetragonal–cubic phase with increase in temperature, as such ions are displaced from their positions to new sites due to the thermal energy. In the present case, it is seen that the transition regions are broad, the combined or individual effects of space charge polarization and motion of Ti^{4+} ions may be the cause of the dielectric relaxation. The relaxation disappears when phase transition is complete and the material goes in high symmetry cubic phase as suggested by Marssi *et al* (1998).

3.3 *Ferroelectric phase transition in PLZT x/57/43*

The reciprocals of the dielectric constant ($1/\varepsilon'_\infty$) as a function of T are shown in figure 7, from which we observe significant broadening of the minima and hence the deviation from the normal Curie–Weiss behaviour, $(1/\varepsilon') = (T - T_C/C)$, where C is the Curie constant. The Curie temperatures, T_C, have been obtained from the least square fit of the straight line data at higher temperatures than T_m. For $x = 3{\cdot}0$ at% of La, T_C almost coincides with T_m, whereas an anomalous behaviour has been observed for $x = 12{\cdot}1$ at% of La for which $T_C < T_m$. The transition temperature, T_m and the Curie temperature, T_C, should essentially be the same for a second order phase transition in the material (Jaffe *et al* 1971; Waser *et al* 2005). Hence $x = 3{\cdot}0$ at% of La shows a second order phase transition. Plots of both T_m and T_C with $\log(x)$ are shown in figure 8.

We observe that T_C and Curie constant, C, decreases with La concentration continuously. The Lorentz factor (T_C/C) gives the strength of coupling between dipoles whereas Curie constant is a representative of the magnitude of the dipole moment. The small Lorentz factor means weaker dipole–dipole interaction. This is found to be the case here because the Lorentz factor for $x = 12{\cdot}1$ at% is 0·0002 while for others it is $0{\cdot}0012 \pm 0{\cdot}0002$, as such decrease in T_C with La content indicates suppression of the long range ferroelectric order. Weakening the dipole–dipole interactions results in the formation of smaller sized domains. Dai *et al* (1993) have also shown that at higher La content, the translational symmetry of polarization is disturbed and the local dipole moments with weak coupling between two BO_6 octahedra via A-site cation are established. These weakly cooperating dipole moments produce the diffuse phase transition in the present systems in agreement with the observations of Dai *et al* (1993, 1994) for tetragonal PLZT systems.

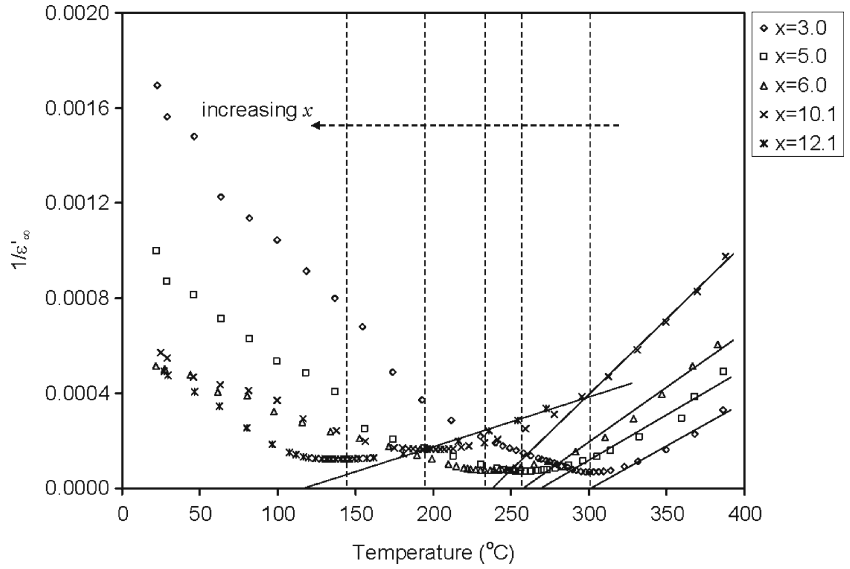

Figure 7. Variation of inverse of the ε'_{∞} with temperature for each composition. The dotted vertical lines show the transition temperature for each composition from right to left respectively which is indicated by arrow in the figure. The solid lines are the linear fits to corresponding data in paraelectric region. Arrow indicates the direction of increasing concentration of La in base PZT.

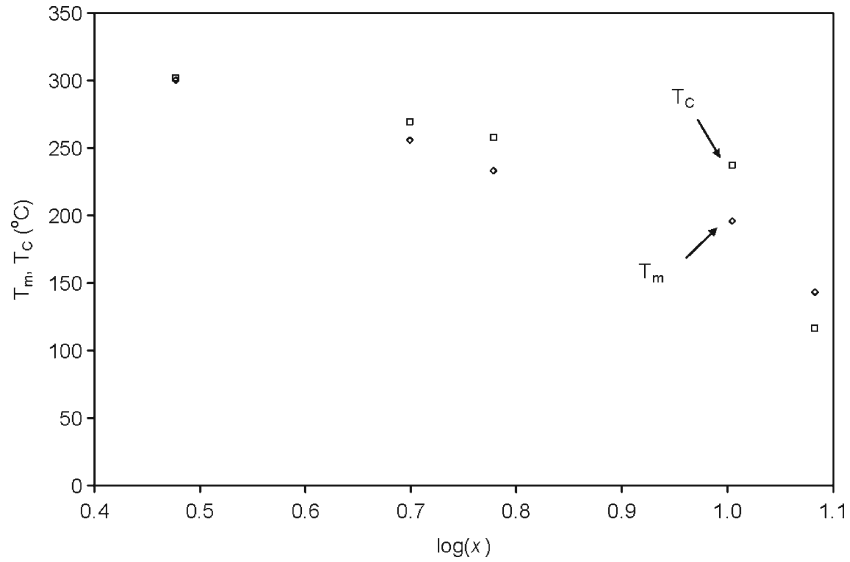

Figure 8. Concentration dependence of T_{m} and extrapolated Curie temperature, T_{C}, for La-doped PZT.

The diffuse type ferroelectric phase transition study may be analysed by a quadratic relation between dielectric constant and temperature (Kirillov and Isupov 1973)

$$\frac{\varepsilon'_{\mathrm{m}\infty}}{\varepsilon'_{\mathrm{m}}} = 1 + \frac{(T - T_{\mathrm{m}})^2}{2\delta^2}, \tag{3}$$

where $\varepsilon'_{\mathrm{m}\infty}$ is the value of dielectric constant at T_{m}, $\varepsilon'_{\mathrm{m}}$ the dielectric constant at T above T_{m} and δ measures the degree of diffuseness in the phase transition. The plots of normalized dielectric constant, $\varepsilon'_{\mathrm{m}\infty}/\varepsilon'_{\mathrm{m}}$ vs square of normalized temperature $(T - T_{\mathrm{m}})^2$ in the paraelectric region are shown in figure 9 from which values of the diffuseness parameter δ are determined and listed in table 4. The continuous increase in δ reveals the increased broadening during the phase transitions from ferroelectric to paraelectric regions with La concentration.

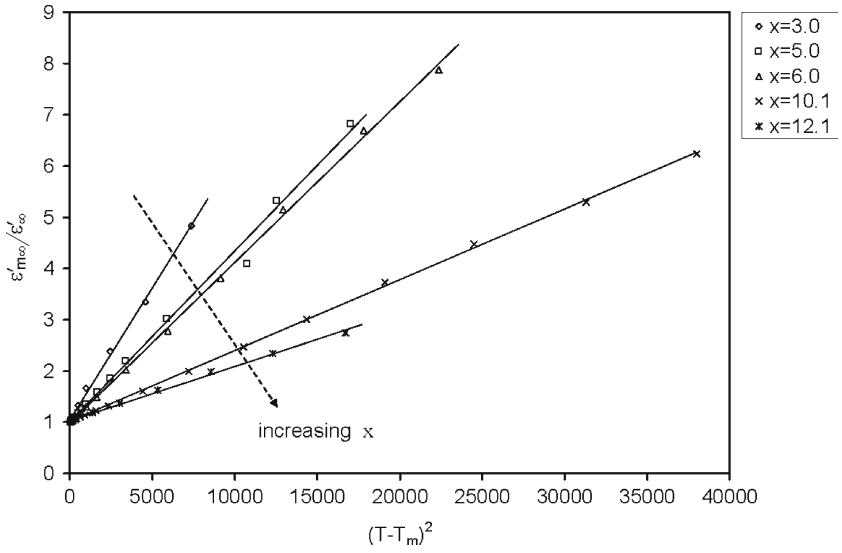

Figure 9. Variation of normalized dielectric constant, $\varepsilon'_{m\infty}/\varepsilon'_{\infty}$, in paraelectric region vs square of normalized temperature for all compositions. The solid straight lines are the linear fits for the corresponding data. The arrow indicates increasing direction of La concentration in base PZT.

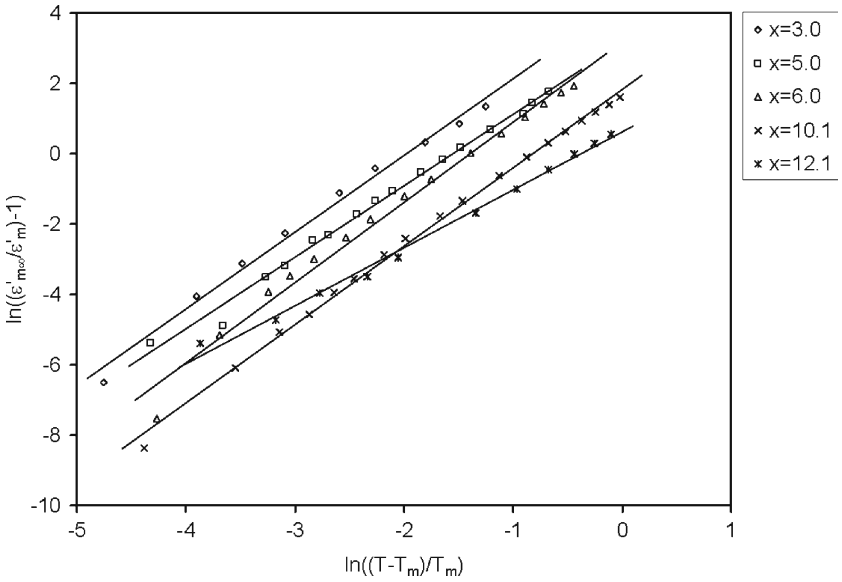

Figure 10. Plot of ln $((\varepsilon'_{m\infty}/\varepsilon'_{m}) - 1)$ vs ln $((T - T_m)/T_m)$ in paraelectric region for various compositions of PLZT.

Table 4. Values of γ and δ obtained from linear fitting of data shown in figure 10.

x (at% of La)	γ (Eqn. 4)	δ (Eqn. 4)	δ(°C) (Eqn. 3)
3·0	2·18	24·5	31·1
5·0	2·03	37·3	38·7
6·0	2·28	33·6	39·9
10·1	2·23	55·7	60·6
12·1	1·65	74·4	68·7

Equation (3) has been further generalized for the materials which do not follow the quadratic behaviour by Martirena and Burfoot (1973)

$$\frac{\varepsilon'_{m\infty}}{\varepsilon'_{m}} = 1 + \frac{T_m^2}{2\delta^2}\left(\frac{T - T_m}{T_m}\right)^{\gamma}. \tag{4}$$

The plots of ln $((\varepsilon'_{m\infty}/\varepsilon'_{m}) - 1)$ vs ln $((T - T_m)/T_m)$ are shown in figure 10 from which γ and δ are obtained (table 4). The parameter, γ, determines the degree of dielectric relaxation in a relaxor ferroelectric material (Cheng *et al* 1997).

The value of $\gamma > 2$, except for $x = 12{\cdot}1$ at% of La for which $\gamma < 2$. Such a behaviour has also been reported by other workers (Stenger and Burggraaf 1980; Arora *et al* 1992).

The domain like transition has been reported in PLZTs (Shemin *et al* 1988; Li *et al* 1995). Based on the transmission electron microscopy (TEM) observations, Li *et al* (1995) proposed domain-like states with increasing La content in PZT whereas at low La content, PLZT behaves like a normal ferroelectric material. Stenger and Burggraaf (1980) proposed the compositional and polarization fluctuations present in the ferroelectric materials but they found that the compositional fluctuations can hardly explain the diffuse phase transition. Cross (1987) suggested that the fluctuations in polarization are dynamical above T_C having significant rms polarization. Viehland *et al* (1992) reported that the deviation from Curie–Weiss law is due to correlations between the superparaelectric regions. Dai *et al* (1994) reported that in case of PLZT 8/40/60 the diffuse type dielectric behaviour is obtained without indication of the relaxor. They further proposed that La in PZT breaks the long range Coulomb interactions which are responsible for spontaneous polarization below T_C. As such the nano sized ferroelectric domains are formed at high La content rather than microdomains.

4. Conclusions

The dielectric response of PLZT compositions x/57/43 has been studied as a function of temperature and frequency. The non-dispersive and dispersive nature of dielectric behaviour has been observed in the studied compositions. The universal dielectric behaviour is obeyed below and above the dispersive region.

A relaxation process is observed in all the samples of PLZT in the low frequency region below 1 kHz with a high value of distribution parameter h. The activation energies of relaxation and conduction processes are calculated and found to be comparable.

The phase transition study of PLZT composition with $x = 3{\cdot}0$ at% of La reveals a second order phase transition. The variation of either T_m or T_C is non-linear with x, though the values of both characterizing temperatures decrease with increasing La concentration. Deviation from Curie–Weiss behaviour along with the diffuse phase transition is observed for all the compositions, the diffuseness increases with increasing La concentration and is found to be a maximum for $x = 12{\cdot}1$ at% of La. The diffuseness in the dielectric behaviour is attributed to the formation of weakly coupled submicron sized polar domains.

Acknowledgements

One of us (AKS) is thankful to the Council of Scientific and Industrial Research (CSIR), New Delhi, for the grant of a Senior Research Fellowship. He also gratefully acknowledges Dr Ashok K Chauhan, Amity University, Noida, for his support.

References

Ang C, Yu Z and Cross L E 2000 *Phys. Rev.* **B62** 228
Arora A K, Tandon R P and Mansingh A 1992 *Ferroelectrics* **132** 9
Bidault O, Goux P, Kchikech M, Belkaoumi M and Maglione M 1994 *Phys. Rev.* **B49** 7868
Bokov A A and Ye Z G 2006 *J. Mater. Sci.* **41** 31
Buixaderas E, Kamba S and Petzelt J 2004 *Ferroelectrics* **308** 131
Cheng Z Y, Katiyar R S, Yao X and Guo A 1997 *Phys. Rev.* **B55** 8165
Cole K S and Cole R H 1942 *J. Chem. Phys.* **10** 98
Cramer C and Buscher M 1998 *Solid State Ion.* **105** 109
Cross L E 1987 *Ferroelectrics* **76** 241
Dai X, DiGiovanni A and Viehland D 1993 *J. Appl. Phys.* **74** 3399
Dai X, Xu Z and Viehland D 1994 *Philos. Mag.* **B70** 33
Dellis J L, Dallennes J, Carpentier J L, Morellc A and Farhi R 1994 *J. Phys. Condens. Matter* **6** 5161
Durand B G, Taillades A, Pradel M, Ribes J, Badot C and Belhadj N – Tahar 1994 *J. Non Cryst. Solids* **172–174** 1306
Dyre J C and Schroder T B 2000 *Rev. Mod. Phys.* **72** 873
Gupta S M, Li J F and Viehland D 1998 *J. Am. Ceram. Soc.* **81** 557
Haertling G H 1999 *J. Am. Ceram. Soc.* **82** 797
Jaffe B, Cook W R and Jaffe H 1971 *Piezoelectric ceramics* (London: Academic Press)
Jonscher A K 1977 *Nature* **267** 673
Kajokas A, Matulis A, Banys J, Mizaras R, Brilingas A and Grigas J 2001 *Ferroelectrics* **257** 69
Kamba S *et al* 2000 *J. Phys.: Condens. Matter* **12** 497
Kirillov V V and Isupov V A 1973 *Ferroelectrics* **5** 3
Kutnjak Z, Filipic C, Pirc R, Levstik A, Farhi R and Marssi M El 1999 *Phys. Rev.* **B59** 294
Lakatos A I and Abkowitz M 1971 *Phys. Rev.* **B3** 1791
Lee W K, Liu J F and Nowick A S 1991 *Phys. Rev. Lett.* **67** 1559
Li J F, Dai X, Chow A and Viehland D 1995 *J. Mater. Res.* **10** 926
Lin H T, Aken D C V and Huebner W 1999 *J. Am. Ceram. Soc.* **82** 2698
Marssi M El, Farhi R, Dellis J L, Glinchuk M D, Seguin L and Viehland D 1998 *J. Appl. Phys.* **83** 5371
Martirena H T and Burfoot J C 1973 *Ferroelectrics* **7** 151
Schmitt H and Dorr A 1989 *Ferroelectrics* **93** 309
Shemin F, Jiawen H and Xi Y 1988 *Ferroelectrics* **77** 181
Shukla A K 2007 *Dielectric studies on ceramics*, D. Phil. Thesis, University of Allahabad, Allahabad
Shukla A K, Agrawal V K, Soni N C, Singh D P, Singh J and Srivastava S L 2004 *Ferroelectrics* **308** 67
Shukla A K, Agrawal V K, Das I M L, Singh J, Singh D P and Sood K N 2006 *Phase Trans.* **79** 875
Shukla A K, Agrawal V K, Das I M L, Singh J and Srivastava S L 2010 *Bull. Mater. Sci.* **33** 383
Stenger C G F and Burggraaf A J 1980 *J. Phys. Chem. Solids* **41** 25
Tan Q and Viehland D 1996 *Phys. Rev.* **B53** 14103
Uchino K 2008 *J. Electroceram.* **20** 301
Viehland D, Jang S J, Cross L E and Wuttig M 1992 *Phys. Rev.* **B46** 8003
Volkov A A, Ritus A I and Khvalkovskii A V 2003 *Ferroelectrics* **285** 219
Waser R, Bottger U and Tiedke S (ed.) 2005 *Polar oxides: Properties, characterization and imaging* (Weinheim: Wiley – VCH Verlag GmbH & Co. KGaA)